

Short Communication

Photoinduced Second Harmonic Generation for the In₂O₃ Nanoparticles Embedded into the PMMA Polymers

A.H.Reshak^{1,2,*}, Anshu Singhal³, Sipra Choudhury³, Z. A. Alahmed⁴, A.O.Fedorchuk⁵,
A.Wojciechowki⁶, H. Kamarudin²

¹New Technologies - Research Center, University of West Bohemia, Univerzitni 8, 306 14 Pilsen, Czech Republic

²Center of Excellence Geopolymer and Green Technology, School of Material Engineering, University Malaysia Perlis, 01007 Kangar, Perlis, Malaysia

³Chemistry Division, Bhabha Atomic Research Centre, Trombay, Mumbai – 400085, India

⁴Department of Physics and Astronomy, King Saud University, Riyadh 11451, Saudi Arabia

⁵Lviv National University of Veterinary Medicine and Biotechnologies, Department of Inorganic and Organic Chemistry, Lviv, Ukraine

⁶Electrical engineering Department, Czestohcowa university Technology, Armii Krajowej 17, Czstohcowa, Poland

*E-mail: maalidph@yahoo.co.uk

Received: 19 November 2013 / Accepted: 15 July 2014 / Published: 25 August 2014

PMMA/ In₂O₃ nanocomposite films for photoinduced nonlinear optics were synthesized. 50% (w/v) solution of PMMA (M_w = 100.000) was prepared in chloroform (purity >99%, from SD Fine Chemicals, Mumbai) and stirred for ca 15 h. To the viscous solution so obtained, appropriate quantity of In₂O₃ nanoparticles was added with continuous stirring. The reaction system was sonicated for two hours. The dispersion so obtained was used for formation of PMMA/In₂O₃ nanocomposite films by spin casting the solution on glass substrate at 10 000 rpm for 20 s. The photoinduced optical second harmonic generation was performed by nanosecond Nd:YAG laser using the bicolour laser treatment. The output SHG has shown nonlinear dependence on the In₂O₃ nanoparticles content.

Keywords: Photoinduced second harmonic generation; In₂O₃ nanoparticles; PMMA polymers

1. INTRODUCTION

The In₂O₃ possess a very good magnitude of energy gap equal to about 3.2 eV which do these materials very promising for the optical applications [1]. Particular interest present nanoparticles of these materials [2]. This is caused by their very specific crystallochemistry structure [3]. However,

to decrease processes of the light scattering the corresponding nanoparticles were embedded into the polymer matrices first of all in the PMMA [4]. The role of the polymer matrix leads both to the filler effect as well as to the additional enhancement due to the interface nano-trapping level on the borders nanocrystallite/polymer due to electron-phonon anharmonic interaction [5], and of a huge interest is an effective distance between the particular chromophore and the surrounding polymer [6].

As a consequence in this article we explore optically stimulated second harmonic generation of the In_2O_3 nanoparticles embedded into the PMMA polymer. For this reason we have chosen nanocomposites possessing materials with the three different concentration of the In_2O_3 nanoparticles. Contrary to the earlier works the corresponding nanocomposites were prepared by a nonhydrolytic alcoholysis ester elimination reaction of indium acetate. This way should open a new opportunity for the separation between the nanoparticle and the polymer matrix.

1.1. Synthesis of In_2O_3 nanoparticles

In_2O_3 nanoparticles were prepared by a nonhydrolytic alcoholysis ester elimination reaction of indium acetate. In a typical preparation 0.25 g of indium acetate along with 20 ml oleyl alcohol and 1.3 ml of oleic acid were taken in a 100 ml volume three-necked flask. The reaction flask was evacuated to a vacuum level of 2 mbar and heated slowly to 100 °C and held at this temperature for 30 min. The reaction system was then heated to 220 °C under flowing argon atmosphere and maintained at this temperature for 4 h. The reaction solution was then cooled to 60 °C, and excess of methanol (20 ml) was added to precipitate the nanocrystals. The off white nanoparticles recovered by centrifugation, were dispersed in toluene and precipitated by addition of methanol. The redispersion/precipitation route was repeated twice to remove any unreacted precursors and excess oleic acid/oleyl alcohol. In_2O_3 nanoparticles so obtained were characterized by powder X-ray powder diffraction (XRD), high resolution transmission electron microscopy, FTIR and Raman spectroscopy and were found to be highly crystalline with cubic bixbyite structure with average crystallite sizes of $\sim 9 \pm 3$ nm.

1.2. Synthesis of PMMA/ In_2O_3 nanocomposite films by spin casting

The details about the synthesis and characterization of PMMA/ In_2O_3 nanocomposite films are the following. Brief, 50% (w/v) solution of PMMA ($M_w = 100.000$) was prepared in chloroform (purity >99%, from SD Fine Chemicals, Mumbai) and stirred for ca 15 h [7]. To the viscous solution so obtained, appropriate quantity of In_2O_3 nanoparticles was added with continuous stirring. The reaction system was sonicated for two hours. The dispersion so obtained was used for the formation of PMMA/ In_2O_3 nanocomposite films by spin casting the solution on glass substrate at 10 000 rpm for 20 s. The films so obtained were dried in air and carefully peeled after 2 h. PMMA/ In_2O_3 nanocomposite films consisting of 1, 2 and 5 wt% In_2O_3 , hence forth mentioned as PMMA-IO1, and PMMA-IO2 and PMMA-IO5, respectively, were prepared. The thickness of the produced films was ~ 50 nm. The nanocomposite films have been structurally characterized by X-ray diffraction (XRD), Fourier

transform infrared (FTIR) spectroscopy and atomic force microscopy and the results confirm the incorporation of In_2O_3 nanoparticles in the PMMA matrix.

2. CHARACTERIZATION

Phase purity and structure of the In_2O_3 nanoparticles and the PMMA/ In_2O_3 nanocomposite films were determined by X-ray powder diffraction (XRD) data, which were collected on a Philips X'Pert pro X-ray diffractometer using Cu-K α radiation ($\lambda = 1.5418 \text{ \AA}$) at 40 kV and 30 mA. AFM images were obtained using a scanning probe microscope (NT-MDT model- SPM solver P47) in contact mode using silicon nitride tips.

3. RESULTS AND DISCUSSION

Fig. 1a shows the XRD patterns of the synthesized In_2O_3 nanoparticles. All the observed peaks can be attributed to cubic- In_2O_3 (JCPDS no. 88-2160). The average crystallite size of the nanoparticles as obtained from the full width at half maximum (FWHM) of the (222) Bragg peak using Scherrer equation with a shape factor of 0.9 was found to be $\sim 9 \pm 3 \text{ nm}$. Fig. 1b shows the XRD patterns for pristine PMMA film and the PMMA/ In_2O_3 nanocomposite films. The diffraction pattern of PMMA shows a very broad diffraction peak at $2\theta \sim 16^\circ$, typical of an amorphous material. Two peaks of much lower intensities centered at 30.0° and 42.7° were also observed.² The XRD spectra of the nanocomposites with 1, 2, and 5% weight loading of In_2O_3 nanoparticles show the peaks observed in PMMA together with the peaks of the fillers, the intensity of which increases with increasing contents. The pattern confirms that the In_2O_3 particles are embedded in the polymer matrix.

3.1. Surface morphology of PMMA/ In_2O_3 nanocomposite films

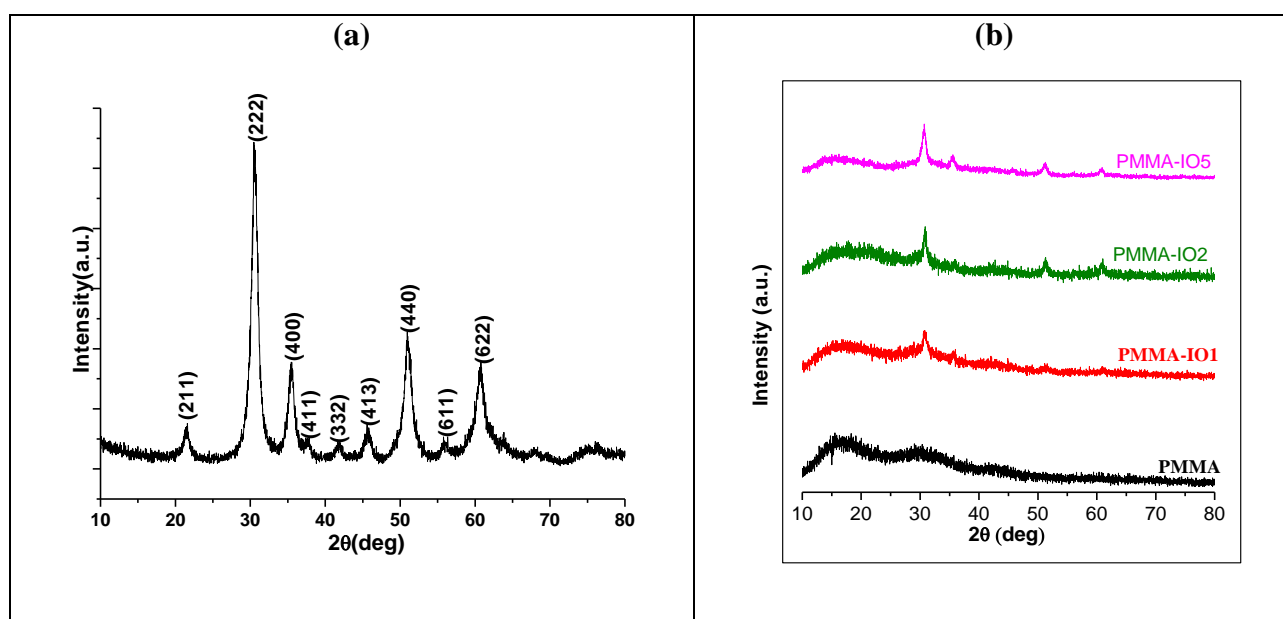


Figure 1. XRD patterns of (a) In_2O_3 nanoparticles and (b) pristine PMMA and PMMA/ In_2O_3 nanocomposite films with different In_2O_3 concentrations.

Surface morphology of the PMMA/In₂O₃ nanocomposite films obtained by spin casting has been investigated by atomic force microscopy (AFM) and the resultant images are shown in Fig. 2. The films are more or less uniform and the statistical root mean square (RMS) roughness values for the PMMA-IO1 (AFM image not shown), PMMA-IO2 and PMMA-IO5 are 2.7 nm, 1.2 nm and 2.16 nm respectively.

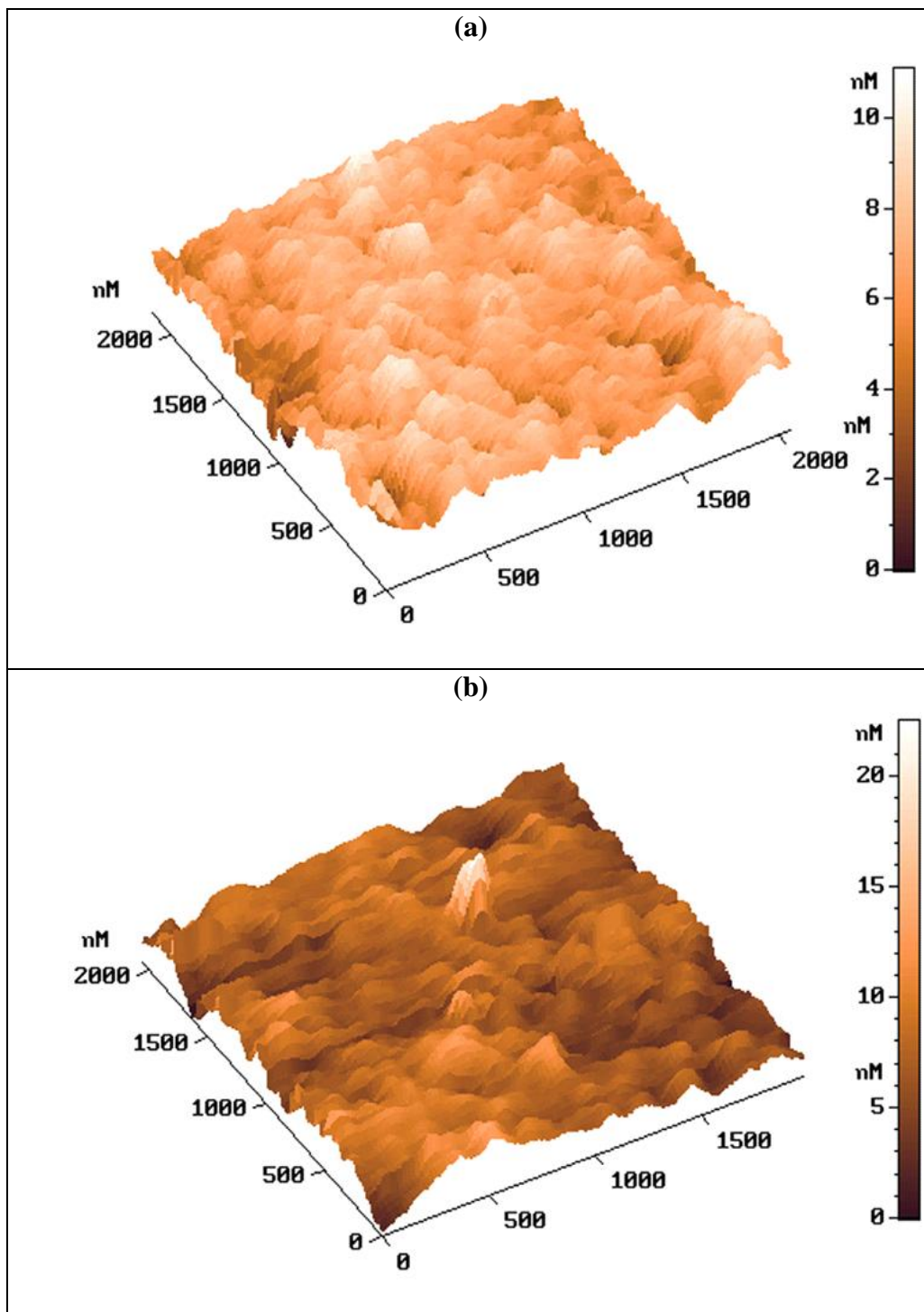


Figure 2. 3D AFM images of spin cast (a) PMMA-IO2 and PMMA-IO5 nanocomposite films

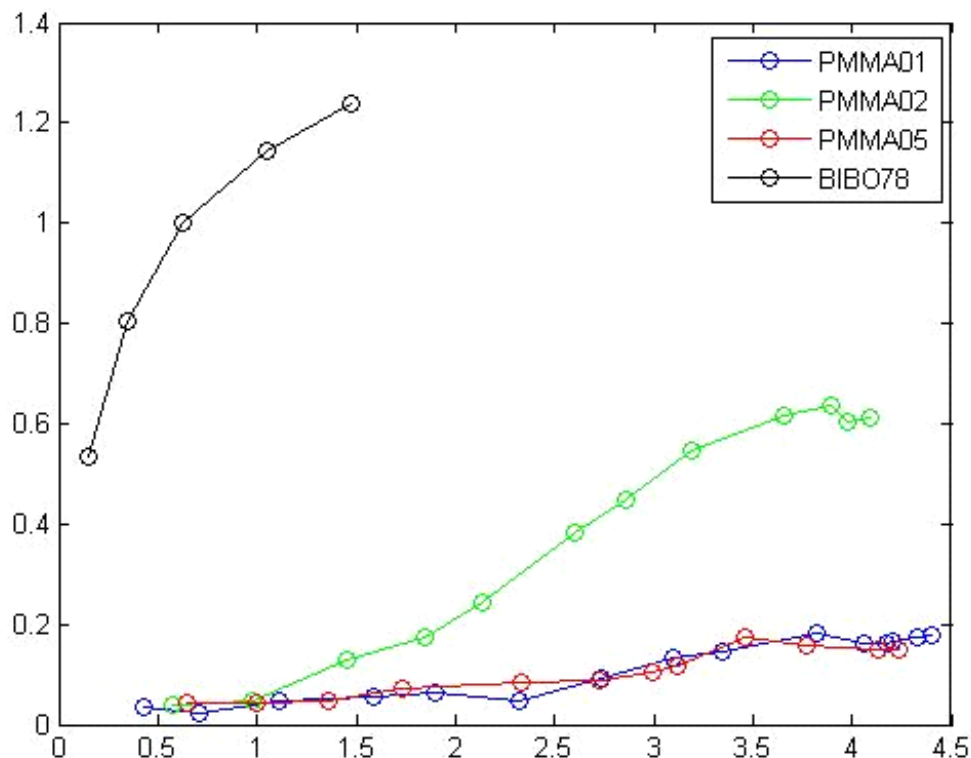


Figure 3. Photoinduced dependence of the second harmonic generation versus the photoinducing power energy in MW/cm².

3.2. Photoinduced second harmonic generation in the In₂O₃/PMMA nanocomposites

The measurements of the photoinduced optical second harmonic generation were performed by a method similar to the described in the ref. 8. The principal results are presented in the Fig. 3. One can see that the maximally achieved SHG was observed for the samples with the In₂O₃ content equal to about 2 %. Such maximum may be caused by optimal magnitude of the effective surfaces separating the nanoparticles and the surrounding polymer. Additionally at this concentration more effective are the electron-phonon anharmonicities [

The absence of peak [321] for XRD patterns of (a) In₂O₃ (Fig.1) confirms on a belonging of the mentioned structure to the structural type (Mn_{0.5}Fe_{0.5})₂O₃, space group *Ia*-3 (206), *a*= 10.077 Å [9]. Standardized crystallographic data for compound In₂O₃ are given in the Table 1.

Table 1. Standardized crystallographic data for compound In₂O₃.

Elements	Wyck.	<i>x</i>	<i>y</i>	<i>z</i>
O	48 <i>e</i>	0.0956	0.36	0.132
In1	8 <i>a</i>	0	0	0
In2	24 <i>d</i>	0.2835	0	1/4

The crystalline structure of the studied compound In_2O_3 by us, may be presented as a oxygen-formed cluster, where In atoms are situated in the three-dimensional channels as is shown in the Fig. 4. The surrounding coordination and distances to the oxygen atoms covering the In atoms are given in the Fig. 5.[10]. The In1 atoms possess symmetrical coordination contrary to atoms In2, for which is observed some acentricity in the surrounding oxygen. Moreover, the inter-atomic distances for the nearest atoms possess some dispersion, which also may favour the effects described by the third order tensor components.

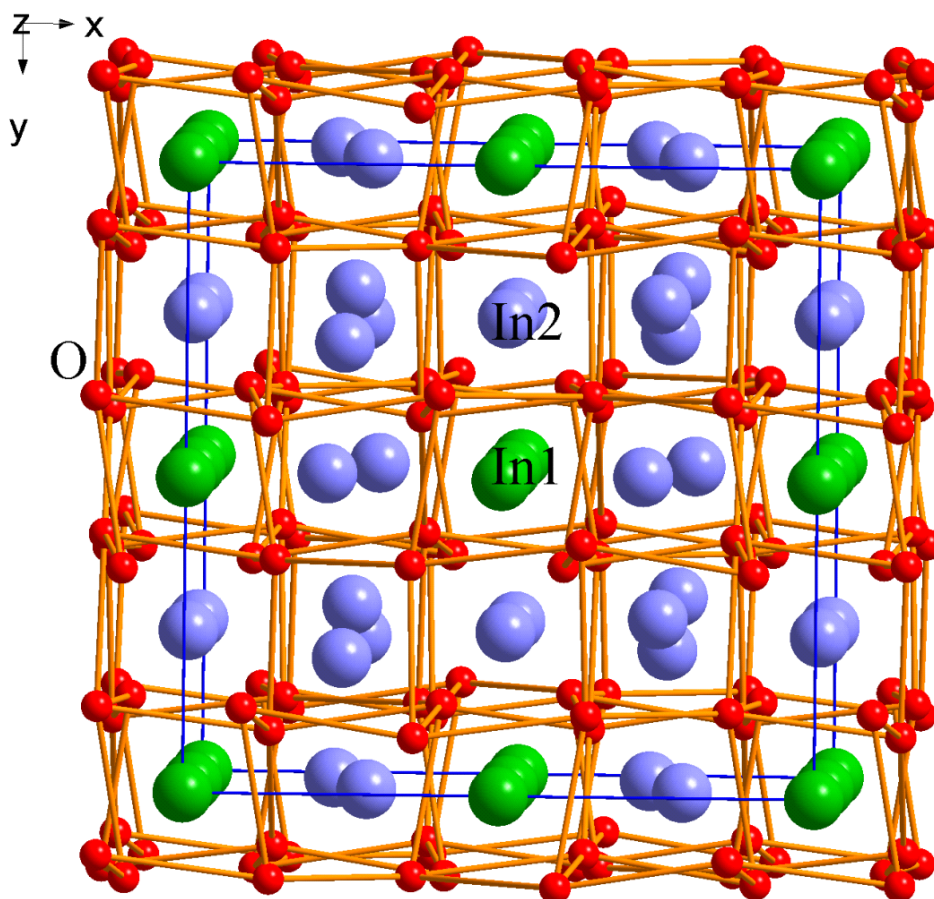


Figure 4. Cluster of oxygen atoms in the In_2O_3

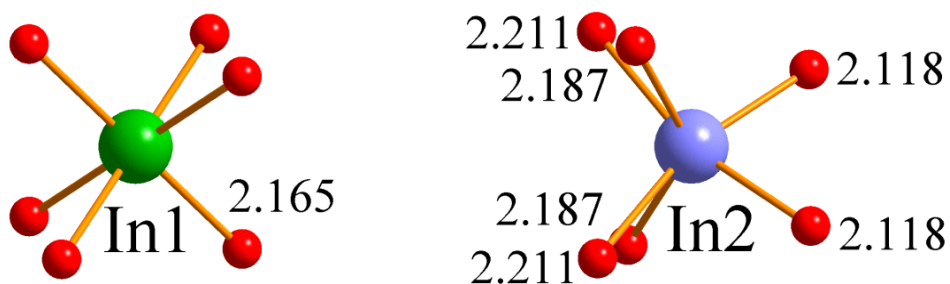


Figure 5. Coordination surrounding and distances (Å) for oxygen atoms in the In_2O_3 .

4. CONCLUSIONS

In₂O₃ nanoparticles were prepared by a nonhydrolytic alcoholysis ester elimination reaction of indium acetate. In a typical preparation 0.25 g of indium acetate along with 20 ml oleyl alcohol and 1.3 ml of oleic acid were taken in a 100 ml volume three-necked flask. The reaction flask was evacuated to a vacuum level of 2 mbar and heated slowly to 100 °C and held at this temperature for 30 min. The reaction system was then heated to 220 °C under flowing argon atmosphere and maintained at this temperature for 4 h. The reaction solution was then cooled to 60 °C, and excess of methanol (20 ml) was added to precipitate the nanocrystals. The off white nanoparticles recovered by centrifugation, were dispersed in toluene and precipitated by addition of methanol. The redispersion/precipitation route was repeated twice to remove any unreacted precursors and excess oleic acid/oleyl alcohol. In₂O₃ nanoparticles so obtained were characterized by powder X-ray powder diffraction (XRD), high resolution transmission electron microscopy, FTIR and Raman spectroscopy and were found to be highly crystalline with cubic bixbyite structure with average crystallite sizes of $\sim 9 \pm 3$ nm. The photoinduced optical second harmonic generation has shown that maximal values were achieved for the composites possessing 2 % of In₂O₃ NP.

ACKNOWLEDGEMENT

The result was developed within the CENTEM project, reg. no. CZ.1.05/2.1.00/03.0088, co-funded by the ERDF as part of the Ministry of Education, Youth and Sports OP RDI program. Computational resources were provided by MetaCentrum (LM2010005) and CERIT-SC (CZ.1.05/3.2.00/08.0144) infrastructures.

References

1. Z. Galazka, I. Irmischer, M. Pietsch, T. Schulz, R. Uecker, D. Klimm, R. Fornari. *Int. J. Electrochem. Sci.*, 8 (2013) 1794 – 1801].
2. N. Siedl, P. Gugel and O. Diwald, *Langmuir*, 29 (20) (2013) 6077–6083
3. S. S. Kim, J. Y. Park, S. W. Choi, H. S. Kim, H. G. Na, J. C. Yang and H. W. Kim. *Nanotechnology* 21(2010) 415502
4. (a) I. V. Kityk, J. Ebothe, Q. Liu, Z. Sun, and J. Fang. *Nanotechnology* (UK), 17 (2006) 1871-1877. (b) I.V. Kityk, Q. Liu, Z. Sun, and J. Fang. *Journ. Phys. Chemistry B*, 110 (2006) 8219-8222. (c) I. V. Kityk, J. Ebothe, S. Tkaczyk, R. Miedzinski, L. Nzoghe-Medome, J. He, X. Sun, K. Sun, J. Lin, J. Fang. *J. Phys., Condensed Matter*, 18 (2007) 016204
5. E. Koscién, J. Sanetra, E. Gondek, B. Jarosz, Optics Communications. 242, (2004), 401-409; E. Koscién, J. Sanetra, E. Gondek, B. Jarosz, *Spectrochimica Acta Part A: Molecular and Biomolecular Spectroscopy*, 61, (2005), 1933-1938
6. I. V. Kityk, M. Makowska-Janusik, E. Gondek, L. Krzeminska, A. Danel, K. J. Plucinska, S. Benet and B. Sahraoui. *J. Phys. Condens. Matter*. 16 (2004) 231-239.
7. (a) A. Singhal, K.A. Dubey, Y.K. Bhardwaj, D. Jain, S. Choudhury and A.K. Tyagi, *RSC Adv.* 3 (2013) 20913 – 20921. (b) M. L. Saladino, T. E. Motaung, A. S. Luyt, A. Spinella, G. Nasillo and E. Caponetti, *Polym. Degrad. Stab.* 97 (2012) 452–459
8. A. Migalska-Zalas, B. Sahraoui, I. V. Kityk, S. Tkaczyk, V. Yuvshenko, J.-L. Fillaut, J. Perruchon, and T.J.J. Muller. *Phys. Rev. (USA)*, B. 71 (2005) 035119.

9. S. Z. Karazhanov, P. Ravindran, P. Vajeeston, A. Ulyashin, T.G. Finstad, H. Fjellvag *Phys. Rev. B: Condens. Matter.* 76 (2007) 075129-1.
10. (a) A. Singhal, K. A. Dubey, Y. K. Bhardwaj, D. Jain, S. Choudhury and A. K. Tyagi, *RSC Adv.*, 3 (2013) 20913 – 20921. (b) M. L. Saladino, T. E. Motaung, A. S. Luyt, A. Spinella, G. Nasillo and E. Caponetti, *Polym. Degrad. Stab.* 97 (2012) 452–459
11. V.T.Adamiv, Ya.V. Burak, I.V.Kityk, J. Kasperczyk, R. Smok, M. Czerwiński. *Optical Materials.* 8 (1997) 207-213.

© 2014 The Authors. Published by ESG (www.electrochemsci.org). This article is an open access article distributed under the terms and conditions of the Creative Commons Attribution license (<http://creativecommons.org/licenses/by/4.0/>).